Crystallization of a large single crystal of cubic insulin for neutron protein crystallography

M. Maeda,[a*] T. Chatake,[a] I. Tanaka,[a] A. Ostermann[b] and N. Niimura[a]

[a]*Neutron Science Research Center, Japan Atomic Energy Research Institute (JAERI), 2-4 Sirakata Shirane, Tokai-mura, Naka-Gun, Ibaraki-ken, 319-1195, Japan,* [b]*Physik-Department E 17 der TUM, James Frank Str., 85747 Garching, Germany*
E-mail: mmaeda@neutrons.tokai.jaeri.go.jp

The growth of a large single crystal of cubic porcine insulin for characterization of hydrogen and hydration in cubic insulin crystals by neutron diffraction analysis is reported. Growth in D_2O was investigated based on the phase diagram for cubic insulin to determine appropriate growth conditions, and a large single crystal was then successfully grown by a dialysis method to a size of $4.0 \times 4.0 \times 1.3$ mm^3. Neutron diffraction analysis of the cubic insulin crystals was carried out using a single-crystal diffractometer at the JRR-3M reactor of the Japan Atomic Energy Research Institute. In preliminary analysis, N_π appears to be protonated and N_τ deprotonated in His5 in the B-chain, whereas both N_π and N_τ are protonated in His10.

Keywords: crystallization; cubic porcine insulin; phase diagram; neutron protein crystallography.

1. Introduction

Hydrogen atoms and hydration water molecules surrounding protein play important roles in many physiological functions. Neutron diffraction for protein crystallography using a neutron imaging plate (NIP) system has emerged as a powerful method for locating the position of hydrogen (deuterium) atoms and bound water in proteins (Niimura *et al*., 1997, 1999). Several results relevant to hydrogen and hydration in proteins have been obtained using high-resolution neutron diffractometers for biological macromolecules (BIX type) installed at the JRR-3M reactor of the Japan Atomic Energy Research Institute (JAERI) (Niimura *et al*., 1997, 2003a, Maeda *et al*., 2001, Kurihara *et al*., 2001, Ostermann *et al*., 2002, Chatake *et al*., 2002). One of the most limiting factors of neutron protein crystallography is the supply of large single crystals. As a minimum, single crystals larger than 1 mm^3 are necessary for neutron diffraction experiments using BIX instruments because of the weak monochromatized neutron beam employed. It is desirable to make large single crystals larger than 2 mm^3. Therefore, the crystallization of large single crystals represents an important problem to be solved. One solution is to investigate a phase diagram and thereby identify the best conditions for producing crystals appropriate for neutron protein crystallography (Arai *et al*., 2002). The phase diagram provides a guideline for making large, high-quality single crystals for diffraction study.

This paper reports the crystallization of a large single crystal of cubic porcine insulin for neutron protein crystallography based on this phase-diagram approach. Three zones in the phase diagram are investigated by a batch method: an undersaturation zone, a metastable zone, and a nucleation zone. The conditions for producing a single crystal appropriate for neutron protein crystallographic analysis are identified, and a large single crystal of cubic porcine insulin crystal is produced.

The structure of this crystal (space group $I2_13$, $a = b = c = 78.9$ Å; $\alpha = \beta = \gamma = 90°$) was initially studied by x-ray structural analysis (Dodson *et al*., 1978) and the results refined to 1.7 Å resolution (Badger *et al*., 1991), through which it has been revealed that cubic insulin crystal contains a solvent volume of 65% and has multiple hydration layers (Badger *et al*., 1993). Crystallographic studies of pH-dependent structural changes in the protein have also been carried out using cubic insulin crystals (Gursky *et al*., 1991,1992; Diao, 2003).

The structure of rhombohedral crystals of 2Zn insulin (space group R3, $a = b = 82.5$ Å, $c = 34.0$ Å; $\alpha = \beta = 90°$, $\gamma = 120°$) was initially solved at 2.8 Å resolution (Adams *et al*., 1969; Blundell *et al*., 1971). The structure of 2Zn insulin crystals has subsequently been refined and analyzed at 1.5 Å resolution (Baker *et al*., 1988). Recently, the structure of T6 (2Zn) human insulin has been determined at 120 K and refined to 1.0 Å resolution (Smith *et al*., 2003). The first neutron protein crystallography of 2Zn insulin was reported at 2.2 Å resolution (Wlodawer *et al*., 1989). However, to the best of the authors' knowledge there have been no reports of the structure of cubic insulin crystals by neutron protein crystallography.

In this study, a large single crystal of cubic porcine insulin is grown and characterized by neutron protein crystallography for the first time. The preliminary results of analysis are presented in this paper.

2. Experimental

2.1. Insulin solution in D_2O

Porcine insulin was purchased from Wako Pure Chemicals Industries, Ltd. For neutron diffraction analysis, it is necessary to avoid strong backgrounds due to the incoherent neutron scattering of H atoms. This effect can be partially overcome either by growing or soaking the crystals in a D_2O solution. This treatment brings about the replacement of some of the hydrogen atoms bound to nitrogen and oxygen (exchangeable hydrogens) with deuterium. In this study, cubic porcine insulin crystal was grown in D_2O. Insulin readily dissolves in pure water with the addition of ammonium hydroxide (McPherson, 1994).

2.2. Phase diagram investigation for the nucleation zone

Crystals of cubic porcine insulin were grown by a batch method using a 24-well plate. The protein concentration was varied from 5 to 25 mg ml^{-1}. The precipitant (Na_2HPO_4) concentration was varied from 0.05 to 0.25 M in the presence of 0.01 M Na_3EDTA, at a total volume of 500 µl (pD 9). The mixtures were filtered through a Millipore 0.22-µm filter unit and placed in an incubator at 298 K (Dodson *et al*., 1978).

2.3. Phase diagram investigation for the undersaturation and metastable zones

In order to investigate the undersaturation and metastable zones, crystals of cubic porcine insulin were dropped into a crystallization solution of different concentrations of solute (insulin) and precipitant (Na_2HPO_4). If the crystal dissolved, the solution condition corresponded to the undersaturation zone, and if the crystal did not dissolve, the solution condition was in the metastable zone.

2.4. Dialysis method

Crystals were grown by a dialysis method in a commercially available micro-dialysis chamber with dialysis membrane attached to the bottom. The protein solution and crystals could be easily observed from the bottom of the chamber. The cubic porcine insulin was dissolved in D_2O with ammonium hydoroxide (0.5 M), and the insulin concentration was varied from 5 to 25 mg ml^{-1} in 500 µl of

internal solution. The protein solution was filtered through a Millipore 0.22 μm filter. The precipitant (Na_2HPO_4) concentration in the outer solution was varied from 0.05 to 0.25 M in the presence of 0.01 M Na_3EDTA. A total volume of outer solution was 2.5 ml (pD 9). The dialysis setup was shielded by a vessel to prevent air contamination and placed in the incubator at 298 K (Dodson *et al*., 1978).

2.5. Data collection

2.5.1. X-ray data collection and reduction

After growing the cubic porcine insulin crystal in D_2O, the crystal structure was investigated by x-ray analysis to obtain an initial model for neutron protein crystallography. The diffraction data for cubic porcine insulin was recorded on a Mac Science DIP-2020 diffractometer with rotating anode x-ray generator operated at 50 kV and 100 mA. The diffraction images were processed and scaled using the programs *DENZO* and *SCALEPACK* (Otwinowski & Minor, 1997).

2.5.2. Neutron data collection and reduction

Neutron diffraction experiments were carried out at room temperature using the BIX-3 single-crystal neutron diffractometer (Tanaka *et al*., 2002) installed at the JRR-3M reactor of JAERI (neutron wavelength 2.9 Å). The crystal was sealed in a quartz capillary for measurement. The step scanning method (0.3°) was used for data collection. The collection time per frame was 55 min, and a total of 300 frames (corresponds to 90° crystal rotation) were collected. The *HKL* software package (*DENZO* and *SCALEPACK*) was used for data processing and scaling.

3. Results and discussion

3.1. Crystallization

Figure 1 shows the phase diagram for cubic insulin versus Na_2HPO_4 concentration. Circles indicate the condition at which crystal nucleation occurs, and triangles indicate the metastable zone where crystals grow when seed crystals exist, but nucleation does not occur. Crosses indicate the region in which crystals do not appear and existing crystals are dissolved, corresponding to the undersaturation zone. The dotted and solid curves denote the boundaries between the metastable and nucleation zones, and between the metastable and undersaturation zones, respectively.

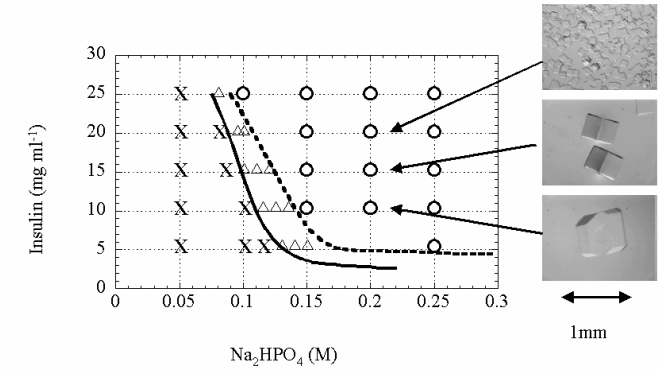

Figure 1
Phase diagram for cubic porcine insulin vs Na_2HPO_4 concentration in D_2O. Insert shows crystals obtained under various supersaturated conditions.

Some examples of insulin crystals grown at different conditions are shown in the insert of Fig. 1. In the batch method, the largest crystal (1 mm^3) was obtained using a protein solution at 10 mg ml^{-1} in 0.2 M Na_2HPO_4. However, it proved difficult to obtain single crystals larger than 2 mm^3 using the batch method because growth of large crystals requires much higher insulin concentrations than possible within this phase diagram. Nevertheless, the phase diagram provides a guideline for conditions suitable for growing single crystals of cubic porcine insulin larger than 2 mm^3 by dialysis.

The speculated process of cubic porcine insulin crystallization for the growth of a large crystal proceeds in the phase diagram as shown in Fig. 2. First, the insulin solution in the undersaturation zone (1) moves toward the nucleation zone (2) through the metastable zone as the precipitant concentration increases by permeation of the precipitant through the membrane, leading to the start of crystallization. The insulin concentration then decreases and the solution moves toward the metastable zone (3). As crystallization continues, the insulin concentration decreases further, and the resultant solution condition moves through the metastable zone, corresponding to the slow growth of crystals without nucleation of new crystals.

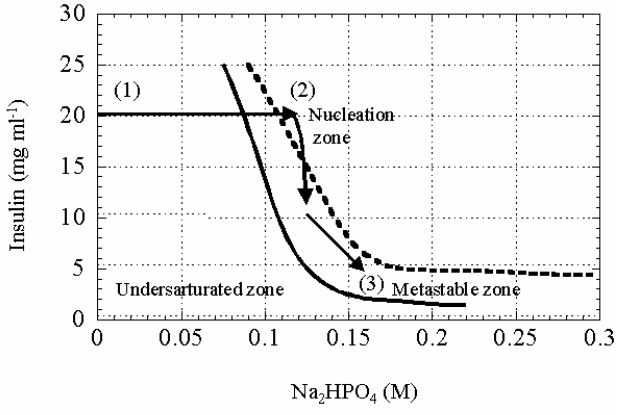

Figure 2
Suggested growth process for large single crystals of cubic porcine insulin.

Several conditions of dialysis were investigated, and the largest crystal was obtained using a protein solution of 20 mg ml^{-1} in 0.2 M Na_2HPO_4. Figure 3 shows the best result of cubic porcine insulin crystal grown in D_2O by dialysis using a dialysis membrane with a molecular weight cut-off (MWCO) of 1000 Da. The largest crystal was $4.0 \times 4.0 \times 1.3$ mm^3 in volume.

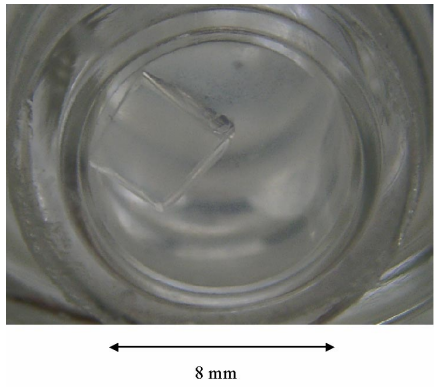

Figure 3
Largest crystal of cubic porcine insulin grown in D_2O by the dialysis method (MWCO: 1000 Da).

Using a dialysis membrane with MWCO of 2000 Da gave an insulin crystal larger than 2 mm^3, but several small insulin crystals also appeared during crystallization, as shown in Fig. 4. This means that the solution condition shifted from metastable to the neucleation zone in the insulin phase diagram during crystallization due to the high permeability of precipitant ions across the 2000 Da membrane.

Thus, a large single crystal suitable for neutron diffraction experiments was successfully prepared by this phase diagram technique.

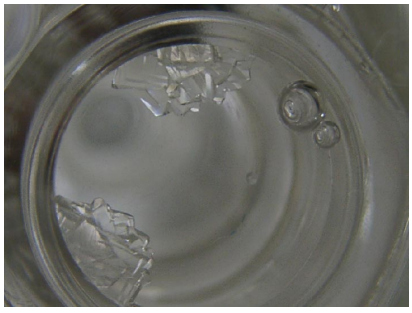

Figure 4
Crystals of cubic porcine insulin grown in D_2O by dialysis using a 2000-Da membrane.

3.2. Preliminary refinement

3.2.1. Initial model by x-ray analysis

Crystallographic refinement was performed using *CNS* (Brünger, *et al*., 1998). A total of 7% randomly selected reflections were used for the calculation of $R_{free.}$ The program *TURBO-FRODO* (Rousel & Cambillau, 1991) was used for viewing electron-density maps and model building. The previously determined structure of cubic porcine insulin (Badger & Dodson, 1991; PDB code 9INS) at 1.7 Å resolution was used for the initial phasing of the data set. The cell constant was set at $a = b = c = 78.90$ Å, and all water molecules in the first model in 9INS were omitted. The final values of $R = 17.84\%$ and $R_{free} = 20.38\%$ were obtained in the resolution range 10.0-1.9 Å.

3.2.2. Neutron analysis

Structure refinement was carried out using *CNS*. The topology and parameter files were modified for neutron crystallography to include hydrogen and deuterium atoms (Ostermann *et al*., 2002). The cubic insulin structure determined by x-ray analysis at 1.9 Å resolution was used as the initial model. The cell constant was set at $a = b = c = 78.92$ Å, and it was assumed that hydrogen atoms bound to carbon atoms were not replaced by deuterium. Hydrogen atoms bound to nitrogen and oxygen were not included in the initial model, and all water molecules were excluded from the model.

Reflection data of between 10.0 and 1.6 Å resolution with $F_{obs} > 2.0\sigma$ (F) were used for refinement. Nuclear density maps ($2|F_o|-|F_c|$ and $|F_o|-|F_c|$) were calculated using 10.0 - 1.6 Å data. Figure 5 shows the *d*-spacing dependence of the completeness of the reflection for various $I/\sigma(I)$ using the result of *SCALEPACK*. The completeness in *d*-spacing from 2.17 to 2.02 Å and from 1.66 to 1.60 Å were 80% and 40%, respectively. The use of high-resolution data was found to afford a better model, even though the completeness of the data set was not high (Niimura & Chatake, 2003b). As representative examples, the $2|F_o|-|F_c|$ nuclear density maps for the side chains of Tyr19 in the A-chain at resolutions of 2.0 and 1.6 Å are shown in Fig. 6. Obviously, the better model was obtained using a resolution of 1.6 Å. Therefore, reflection data of 10.0 to 1.6 Å resolution was used in the map calculation. In the refinement, the positions of exchangeable hydrogen atoms of each amino acid residues were identified using the $2|F_o|-|F_c|$ and $|F_o|-|F_c|$ nuclear density maps. Hydrogen and deuterium atoms could be identified as negative and positive peaks in the $2|F_o|-|F_c|$ map, respectively. Water molecules (D_2O) were also identified using the maps. This analysis is continuing and will be reported in the future.

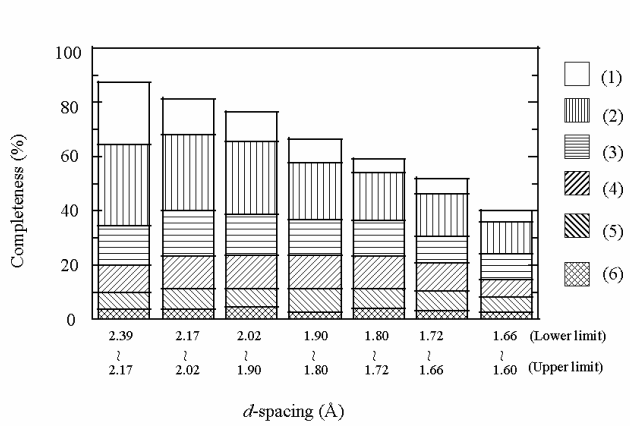

Figure 5
d-spacing dependence of the completeness of reflection for various $I/\sigma(I)$. Numbers correspond to (1) $I/\sigma(I) \geq 10$, (2) $10 > I/\sigma(I) \geq 5$, (3) $5 > I/\sigma(I) \geq 3$, (4) $3 > I/\sigma(I) \geq 2$, (5) $2 > I/\sigma(I) \geq 1$, and (6) $1 > I/\sigma(I) \geq 0$.

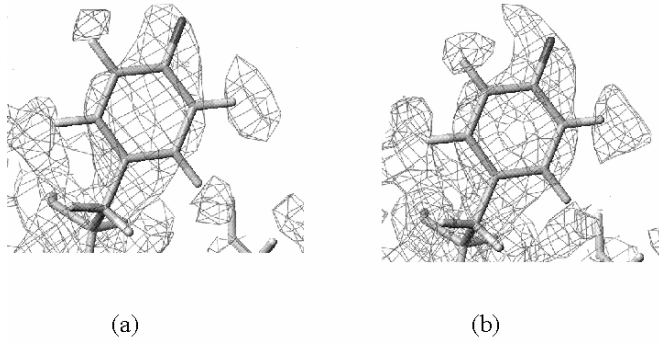

Figure 6
$2|F_o|-|F_c|$ nuclear density map for the side chain of Tyr19 in the A-chain at resolutions of (a) 2.0 Å and (b) 1.6 Å.

3.2.3. Hydrogen of histidine

Protonation and deprotonation of the two nitrogen atoms (N_π, N_τ) in the imidazole ring of histidine are important in discussion of insulin crystals. It is known that His10 in the B-chain (B10 His) is a zinc ion-binding site (Adams *et al*., 1986). Figure 7 shows the $2|F_o|-|F_c|$ positive neutron density map for His5 in the B-chain (B5 His) and His10 in the B-chain (B10 His) of cubic insulin at 1.6 Å resolution. In B5 His, N_π is protonated and N_τ is deprotonated, whereas in B10 His, both N_π and N_τ are protonated.

In the case of 2Zn insulin crystals at pH 6.3, it has been shown that both nitrogen atoms are protonated in B5 His according to the $2|F_o|-|F_c|$ neutron density map (Wlodawer et al., 1989). However, the protonation and deprotonation for B10 His were not described in that paper. This structure of 2Zn insulin has been registered with the Protein Data Bank as PDB entry 3ins (Wlodawer *et al*., 1989). According to the PDB entry, N_π is protonated and N_τ is deprotonated in B10 His. Comparison of cubic insulin crystal and 2Zn insulin crystal by neutron analysis gave the opposite result with respect to the protonation and deprotonation of histidine.

In a study of the relationship between cubic insulin and 2Zn insulin by x-ray analysis, Badger *et al*. (1991) showed that the cubic insulin molecule is significantly more similar to one of the two independent molecules in the 2Zn insulin dimer than the other. In comparison with 2Zn insulin, B10 His is rotated by about 90° in the cubic crystal. Thus, it appears that the dissimilar results obtained for protonation and deprotonation are related to the environment of the binding sites, such as the geometry of hydrogen bonds and the solvent position. If the hydration structures of both crystals that include hydrogen (deuterium) positions can be observed, it is expected that more details will be obtained. The present authors intend to investigate the hydrogen and hydration structure of not only cubic insulin crystals, but also 2Zn insulin crystals, and growth of large single crystals of 2Zn insulin is currently underway. High-resolution neutron diffraction data will be reported in the near future as part of a comparative study of the neutron protein crystallography of cubic insulin and 2Zn insulin.

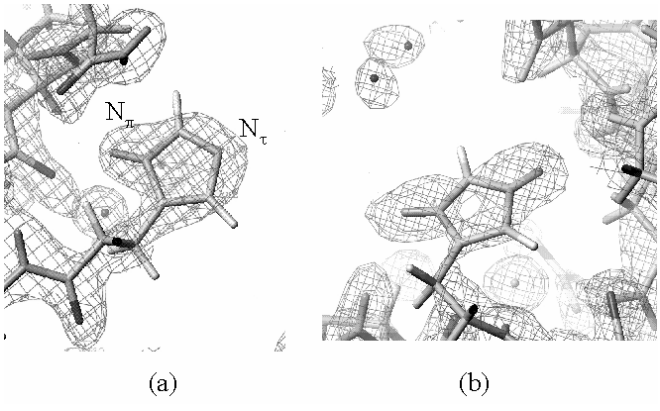

Figure 7
$2|F_o|-|F_c|$ positive nuclear density map of (a) His5 in the B-chain and (b) His10 in the B-chain of cubic insulin.

4. Conclusion

Using a phase diagram technique, a large, high-quality single crystal of cubic porcine insulin suitable for neutron diffraction analysis was successfully prepared. Preliminary analysis of the crystal revealed that N_π is protonated and N_τ is deprotonated in B5 His, whereas both nitrogen atoms are protonated in B10 His.

This work was supported in part by an 'Organized Research Combination System' Grant from the Ministry of Education, Culture, Sports, Science and Technology, Japan.

References

Adams, M. J., Blundell, T. L, Dodson, E. J., Dodson, G. G., Vijayan, M., Baker, E. N., Harding, M. M., Hodgkin, D. C., Rimmer, B. & Sheat, S. (1969). *Nature* (*London*), **224**, 491-495.
Arai, S., Chatake, T., Minezaki, Y. & Niimura, N. (2002). *Acta. Cryst.* D**58**, 151-153.
Badger, J., Harris, M. R., Reynolds, C. D., Evans, A. C., Dodson, E. J., Dodson, G. G., & North, A. C. T. (1991). *Acta Cryst.* B**47**, 127-136.
Badger, J. (1993). *Biophys. J*. **65**, 1656-1659.
Baker, E. N., Blundell, T. L., Cutfield, J. F., Cutfield, S. M., Dodson, E. J., Dodson, G. G., Hodgkin, D. C., Hubbard, R. E., Isaacs, N. W., Reynolds, C. D., Sakabe, K., Sakabe, N. & Vijayan, M. (1988). *Philos. Trans. R. Soc. London, Ser*. B, **319**, 369-456.
Blundell, T. L., Cutfield, J. F., Cutfield, S. M., Dodson, E. J., Dodson, G. G., Hodgkin, D. C., Mercola, D. A. & Vijayan, M. (1971). *Nature* (*London*), **231**, 506-511.
Brünger, A. T., Adams, P. D., Clore, G. M., DeLano, W. L., Gros, P., Grosse-Kunstleve, R. W., Jiang, J.-S., Kuszewski, J., Nilges, M., Pannu, N. S., Read, R. J., Rice, L. M., Simonson, T. & Warren, G. L. (1998). *Acta Cryst*. D**54**, 905-921.
Chatake, T., Kurihara, K., Tanaka, I., Adams, M. W. W., Jenney, F. E., Jr., Tsyba, I., Bau, R. & Niimura, N. (2002). *Appl. Phys.* A**75**, 1-3.
Gursky, O., Badger, J., Li, Y. & Caspar, D. L. D. (1991). *Biophys. J*. **61**, 604-612.
Gursky, O., Badger, J., Li, Y. & Caspar, D. L. D. (1992). *Biophys. J*. **62**, 1210-1220.
Diao, J. (2003). *Acta Cryst*. D**59**, 670-676.
Dodson, E. J., Dodson, G. G., Lewitova, A. & Sabesan, M. (1978). *J. Mol. Biol*. **125**, 387-396.
Kurihara, K., Tanaka, I., Adams, M. W. W., Jenney, F. E., Jr., Moiseeva, N., Bau, R. & Niimura, N. (2001). *J. Phys. Soc. Jpn*., Suppl. A, 7**0**, 400-402.
McPherson, A. (1994). *Crystallization of Biological Macromolecules*. Cold Spring Harbor Laboratory Press. New York : pp. 488-489
Maeda, M., Fujiwara, S., Yonezawa, Y. & Niimura, N. (2001). *J. Phys. Soc. Jpn*. Suppl. A, **70**, 403-405
Niimura, N., Minezaki, Y., Nonaka, T., Castanga, J.-C., Cipriani, F., Hoghoj, P., Lehmann, M. S. & Wilkinson, C. (1997). *Nat. Struct. Biol*. **4**, 909-914.
Niimura, N. (1999). *Curr. Opin. Struct. Biol*. **9**, 602-608.
Niimura, N., Chatake, T., Ostermann, A., Kurihara, K., & Tanaka, I. (2003a). *Z. Kristallogr.* **218**, 96-107.
Niimura, N. & Chatake, T. (2003b). *J. Jpn. Soc. Neutron Sci*. **13**, 47-50.
Ostermann, A., Tanaka, I., Engler, N., Niimura, N. & Parak, F. G. (2002). *Biophys. Chem.* **95**, 183-193.
Otwinowski, Z. & Minor, W. (1997). *Methods Enzymol*. **276**, 307-326.
Rousel, A & Cambillau, C. (1991). *Silicon Graphics Geometry Partners Directory*, pp. 86-89. Mountain View, CA: Silicon Graphics.
Smith, G. D., Pangborn, W. A. & Blessing, R. H. (2003). *Acta Cryst*. D**59**, 474-482.
Tanaka, I., Kurihara, K., Chatake, T. & Niimura, N. (2002). *J. Appl. Cryst.* **35**, 34-40.
Wlodawer, A., Savage, H. & Dodson, G. (1989). *Acta. Cryst.* B**45**, 99-107.